GASMEMS11-7

DSMC SOLUTION FOR THE ADIABATIC AND ISOTHERMAL MICRO/NANO LID-DRIVEN CAVITY

Alireza Mohammadzadeh
Email: a.mohammadzadeh_mec@yahoo.com

Ehsan Roohi
Email: roohi@ae.sharif.edu

Hamid Niazmand
Email: hniazmand@yahoo.com
Department of Mechanical Engineering, Faculty of Engineering.
Ferdowsi University of Mashhad, Mashhad, Iran. P.O.BOX: 91775-1111

Stefan Stefanov
Email: stefanov@imbm.bas.bg
Institute of Mechanics, Bulgarian Academy of Science.
Acad. G. Bontchev str., 1113, Sofia, Bulgaria.

Abstract

We utilized direct simulation Monte Carlo (DSMC) method to investigate the effects of boundary conditions on the thermal characteristic of the micro/nano mid-driven cavity in the slip and transition regimes. Monatomic argon gas confined in micro/nano isothermal and adiabatic lid-driven cavity is considered in this study. It is seen that hydrodynamic flow behaviours are similar for both cases, however, the adiabatic cavity encounters higher temperature rise in comparison to the isothermal cavity. Moreover, the directions of heat flux streamlines are quite different for the two cases. It is seen that in the slip regime the heat flux streamlines are generated from top left corner and are directed toward all walls of the isothermal cavity. In the adiabatic cavity the heat flux streamlines are only directed toward the driven-lid. Finally, the entropy distribution is calculated in the flow field. It is seen that direction of the heat flux streamlines agrees with the direction of the entropy isolines instead of temperature gradients in the domain. Fourier law, which assumes that heat always fluxes from hotter to colder region, loses its validity in the slip regime and beyond.

1. Introduction

The study of gaseous flow in micro and nano scales has been an interesting and appealing topic of researches in recent years. It is well known that the traditional Navier-Stocks-Fourier (NSF) equations lose their promise to describe flow features as characteristic length enters micro range and beyond. Knudsen number, which is defined as the ratio of the mean free path of the fluid to the characteristic length of the flow domain ($Kn=\lambda/L$), is the main tool to determine degrees of gas rarefaction. According to the Kn number range, the state of a gaseous flow can be defined in four different regimes [1]. Firstly, gaseous flow at $Kn < 0.001$ is termed as continuum regime. The NSF equations with no-slip boundary conditions are appropriate and valid in this regime. Secondly, the gaseous flow with Kn number ranges of $0.001 < Kn < 0.1$ is called slip flow. Special treatment must be considered in the NSF equations to capture flow features accurately in slip regime. Transition regime is termed for $0.1 < Kn < 10$. In this regime, the NSF equations lose validity and the well

known first order shear stress and heat flux approximations fail to predict flow behaviour. Flow is considered as free molecular if Kn > 10. Discrete molecular modelling is the main tool to model flow field in all degrees of rarefaction. In this method, the fluid is modelled as a collection of moving molecules which interact through collisions. The DSMC is known as one of the most successful particle simulation methods in analysing the rarefied gaseous flows.

The driven cavity is a common geometry in the industrial application. In spite of the geometrical simplicity, lid-driven cavity can encounter very complex flow features such as compressibility effects and corner eddies. Cooling electronic devices by using lid-driven flows [2] and flow in a short-dwell coater in the production of high-grade paper and photographic film [3] are some applications of such geometry. Mizzi et al. [4] compared the efficiency of continuum approach with DSMC method in the slip and early transition regimes for micro lid-driven cavity. They reported that as the Kn number increases the NSF equations loses their validity especially in the close proximity to the top corners where non-equilibrium effects are stronger. John et al. [5] investigated the effects of top wall speed on the flow characteristic in the micro lid driven cavity by means of the DSMC technique. They claimed that in the transition regime as the lid velocity increases the center of vortex shifts toward right and also upward. John et al. [6] also studied the effect of incomplete surface accommodation on the heat transfer in the lid driven cavity. They reported that incomplete surface accommodation can significantly affect both hydrodynamic and thermal characteristic of the cavity flow.

In this paper the DSMC method is utilized to investigate the effects of boundary conditions on the hydrodynamic and thermal behaviour of the cavity flow. In particular, we focus on the heat flux dependencies on the boundary conditions.

1. GOVERNING EQUATIONS

2.1 The DSMC approach

DSMC is a particle method based on kinetic theory for the simulation of dilute gases. The method is carried out by modelling the gas flow using many independent simulated molecules. These simulated molecules are representatives of a large number of real gas particles in the flow field. The time step Δt in the DSMC method is chosen as small as the positional changes of particles and their collisions could be decoupled for each time step. In order to implement DSMC, flow field must be divided into computational cells. The size of each cell should be small enough to result in small changes in thermodynamic properties across each cell. The cells provide geometric boundaries and volumes, required to sample macroscopic properties. They are also used as a unit where only molecules located within the same cell at a given time are allowed for collision

In the current study the previous code of Roohi and co-workers [7-9] is extended to simulate rarefied flow in the micro/nano cavity. The VHS collision model is used to consider accurate variation of viscosity with temperature. The choice of collision pair is done based on the no time counter (NTC) method. NTC scheme makes the computational time proportional to the number of the simulated particles [1]. Monatomic argon, m=6.63×10-26 Kg and d=4.17×10-10 m is considered as the gaseous medium. In order to ensure the satisfaction of the limits on the cell size, the cell dimensions Δx,Δy are considered 0.1λ and are much smaller than that for most cases. 32 molecules are set in each cell to minimize the scattering noise. All walls are treated as diffuse reflectors using the full thermal accommodation coefficient, α=1. Half-range Maxwellian distribution is used to determine the velocity of reflected molecules. After achieving steady flow condition, sampling of flow properties within each cell is fulfilled during sufficient time period to avoid statistical scattering. All thermodynamic parameters such as temperature, density, and pressure are then determined from this time-averaged data. In order to minimize the scattering in the predicted results, particularly

temperature, a filtering post processor is utilized. In this method the sampled macroscopic properties (F) are averaged over four neighbouring cells, as given below.

3. RESULTS AND DISCUSSION

3.1 Grid independency test & code validation

The micro driven cavity considered in this study is shown in figure 1. Four corners of the cavity is denoted by A, B, C and D. The top driven lid moves in positive x-direction with U_{wall}=100 m/s. Cavity flow at slip and transition regimes, i.e., Kn=0.05, 0.1 and 0.5, is considered. The walls temperature is set to the reference temperature, i.e., $T_w=T_0$=300 K for the isothermal cavity. For the adiabatic cavity all walls except of the driven lid are assumed adiabatic. Modeling a free stream on an adiabatic cavity makes the top wall temperature remains constant at the initial temperature of the flow filed.

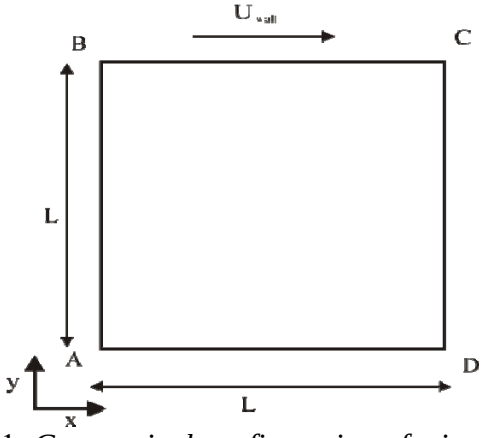

Figure 1: *Geometrical configuration of micro cavity*

A grid independency study was carried out using three grids composed of 50×50, 200×200 and 400×400 cells. Figure 2 shows the vertical component of velocity vector along the horizontal axis of the cavity for this test. The results are numerically equivalent for 200×200 and 400×400 grids; therefore the grid containing 200×200 cell is selected for the reported results in this study.

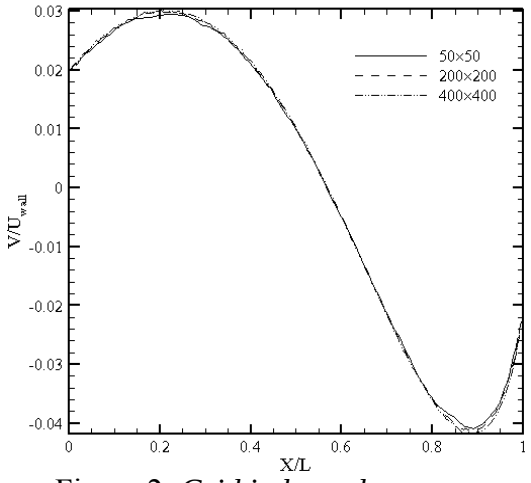

Figure 2: *Grid independency test*

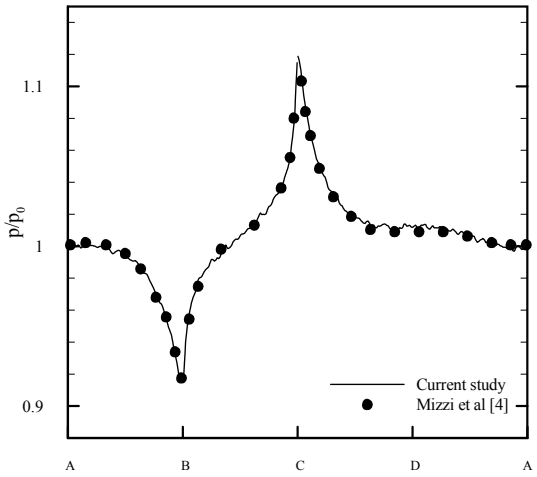

Figure 3: *Comparison of non-dimensional pressure along four walls of the cavity*

In order to access the validity of the DSMC results, predicted pressure at Re= 1.5 and Kn= 0.1 is compared with the reported data of Mizzi et al. [4]. Figure 3 shows the non-dimensional pressure, p/p_0, where p_0 is the initial pressure of the rarefied flow field, for argon flow along four walls of the cavity. It is seen that predicted values by the DSMC code in this study are in good agreement with reported data of Mizzi et al. [4].

3.2 Comparison of the isothermal with adiabatic cavity

Attention is now directed to the comparison of the isothermal cavity with the adiabatic cavity. Figure 4 shows the comparison of predicted horizontal and vertical velocity along the vertical and horizontal centrelines of the cavity. As expected, increasing the Kn number reduces the imposed wall velocity on the domain. It is seen that the boundary condition does not affect the hydrodynamic characteristic of the cavity flow notably.

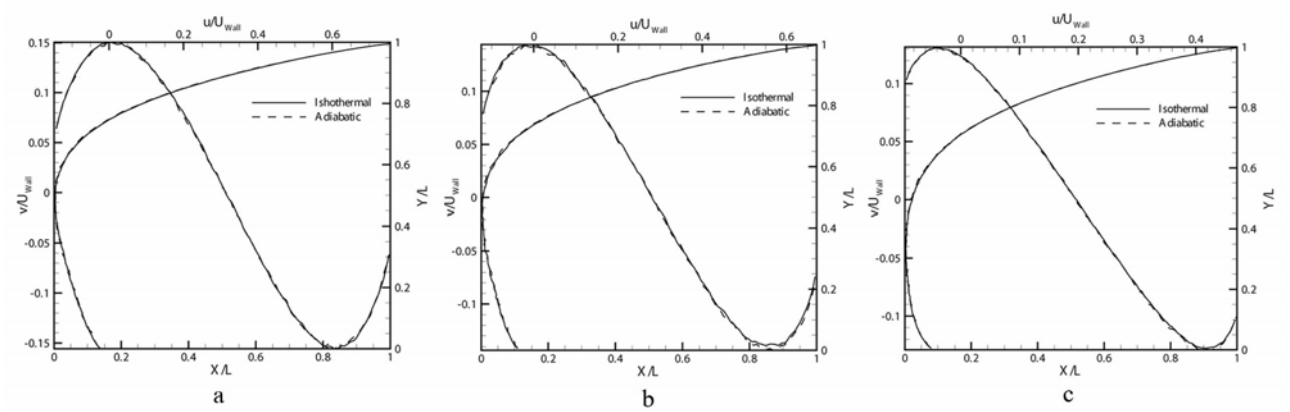

Figure 4: *Comparison of velocity components for the isothermal and adiabatic cavity, a) Kn=0.05, b) Kn=0.1, c) Kn=0.5*

Comparison of flow temperature along the horizontal centreline of the cavity is shown in Fig. 5. It is seen that as the Kn number increases the predicted temperature grows. Increasing the Kn number makes the rarefaction effects pronounce more significantly. This results in higher temperature of the flow near the right side wall. Figure 5 shows that the maximum temperature along the horizontal centreline of the cavity is closer to the right wall for the adiabatic cavity. It shows that the compressibility effect is more notable for this case in comparison to the isothermal cavity.

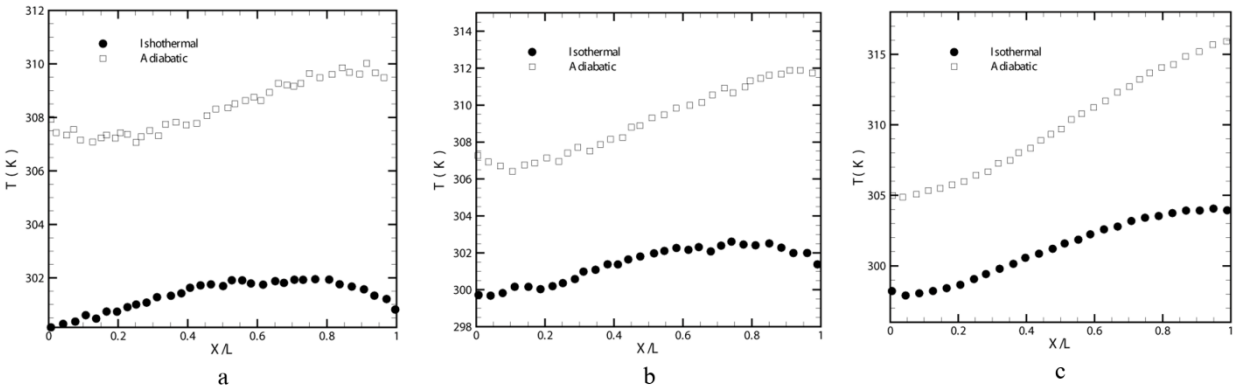

Figure 5: *Comparison of temperature profile along the horizontal centerline for the isothermal and adiabatic cavity, a) Kn=0.05, b) Kn=0.1, c) Kn=0.5*

Figure 6 shows the heat flux streamlines overlaid on the temperature contours. Flow field encounters two mechanisms for transfer of energy in this case. The competition between compressibility effects and viscous dissipation dominate the heat characteristic of the flow. Figure 6.a shows the temperature contour for the isothermal cavity at Kn=0.05. Reduction in flow temperature near the left wall shows that the compressibility effect in this region dominates the heat transfer mechanism. As flow approaches to the right corner, both energy transfer mechanisms work in favour of increasing the flow temperature, thus, the value of maximum temperature is much greater than the initial one. Surprisingly, heat flux streamlines are from the colder region of the cavity to the hotter region. According to the Fourier law, qx=-k∂T/∂x, such direction for the flux of energy is not expected. The heat flux along the horizontal coordinate is given by following molecular dynamic relation:

$$q_x = \frac{1}{2}[\rho(\overline{c^2 u} - \overline{c^2} u_0) - 2p_{xx}u_0 - 2p_{xy}v_0] \qquad (1)$$

where $p_{ij} = \rho\overline{c_i' c_j'}$ is the pressure tensor.

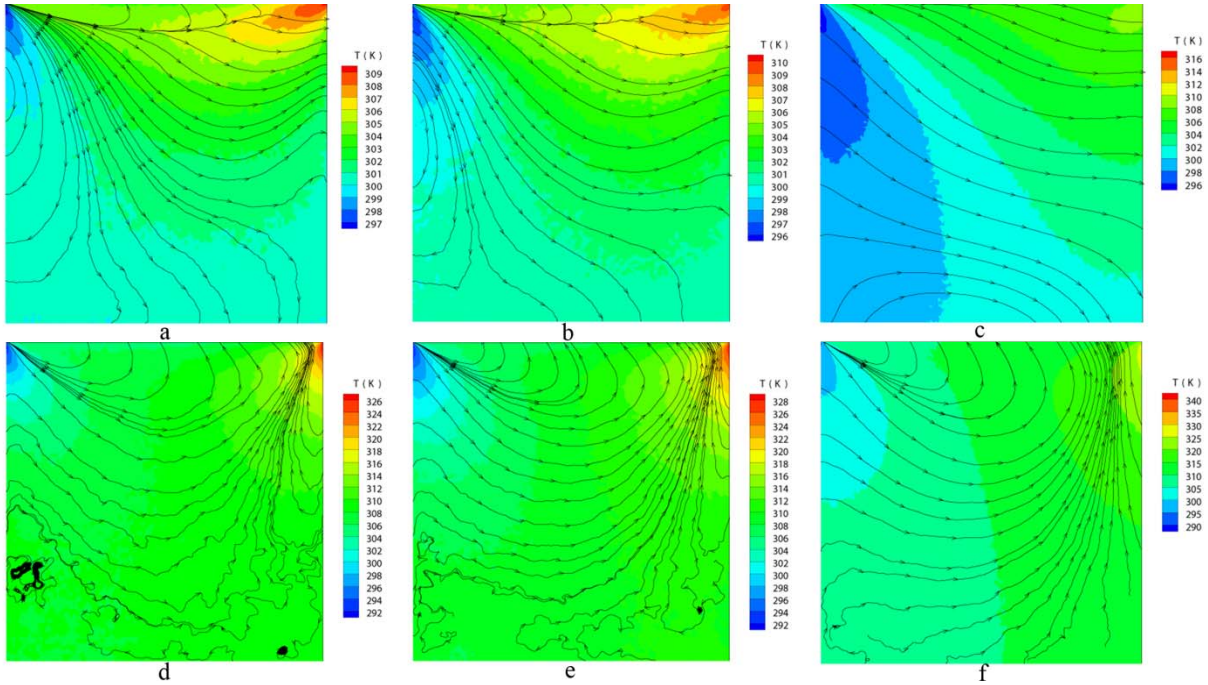

Figure 6: *Heat flux streamlines overlaid on the temperature contour, top row: isothermal cavity, a) Kn=0.05, b) Kn=0.1, c) Kn=0.5, bottom row: adiabatic cavity, d) Kn=0.05, e) Kn=0.1, f) Kn=0.5*

According to Eq. (1), molecular velocity components affect the heat flux direction. Additionally, the results of Mizzi [10] showed that the predicted heat flux direction by the regularized 20-moment method agrees with the DSMC solution. Figure 6.d shows the heat flux direction for the adiabatic cavity. It is seen that the directions of the heat flux are different from the isothermal case. Since the transfer of energy is only possible via the driven lid, all the heat flux lines are directed to this wall. Very similar to the previous case, increasing the Kn number makes the maximum temperature of domain increase and also the energy flux lines become smoother. Smaller minimum temperature of the adiabatic cavity in comparison with the isothermal cavity shows that the compressibility effects are more pronounced for this case. The temperature contour shapes are also different for the two cases.

Figure 6.b shows the heat flux streamlines in the isothermal cavity at Kn=0.1. The heat flux streamlines and temperature contours are quite similar to the case at Kn=0.05, but the maximum and minimum values of temperature change by one degree. As the Kn number increases, the compressibility effect grows. This results in higher temperature value at the top right corner due to the sudden contraction and smaller minimum temperature at the left wall due to the sudden expansion. Flux of energy in the DSMC method is carried out via convection by molecules and their collisions. As the Kn number increases, convection plays a more vital role in the energy transfer in the domain. Figure 6.e shows the temperature contour in the adiabatic cavity at the border of slip regime. The distribution of temperature contour is similar to the case with Kn=0.05. In the lower half of the cavity, where the velocity of molecules is the smallest, the heat flux streamlines change direction instantaneously. Heat flux streamlines in the transition regime is shown in Figure 6.c and Figure 6.f. In this regime higher temperature as a result of greater pressure variation in the flow field is predicted. Moreover, heat flux streamlines are quite smooth in the flow field which indicates that the transfer of energy via convection of molecules predominates in the entire domain.

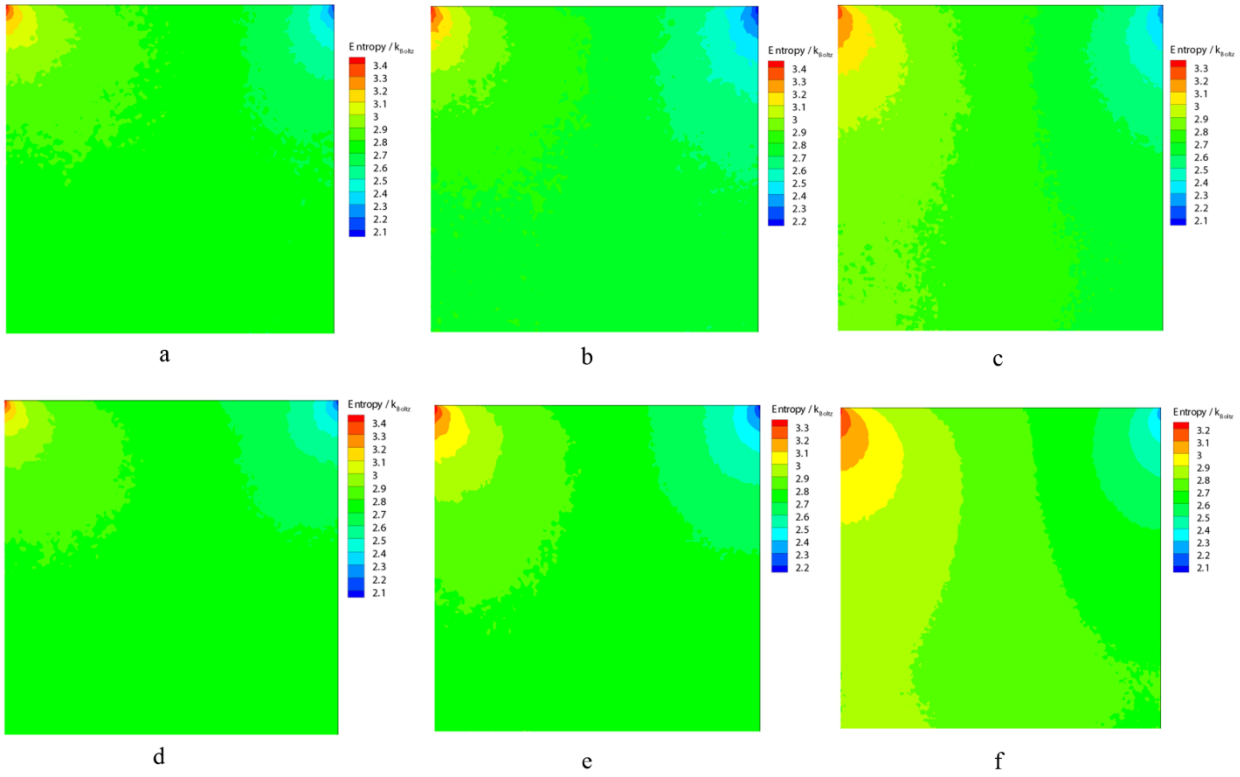

Figure 7: *Entropy contour, top row: isothermal cavity, a) Kn=0.05, b) Kn=0.1, c) Kn=0.5, bottom row: adiabatic cavity, d) Kn=0.05, e) Kn=0.1, f) Kn=0.5*

In order to study the thermal behaviour of the cavity flow more precisely, the entropy distribution in the cavity flow is shown in figure 8. According to the molecular gas dynamic relations, entropy is proportional to the H function is given by [11]:

$$E = -k\sum_{bins}\Delta v\frac{N_h(v)}{N}\ln\frac{N_h(v)}{N} \qquad (2)$$

where Δv is the width of the velocity bin, $N_h(v)$ is the number of particles in the regarding bin and N is the total number of particles in all the velocity bins. It is known that the energy fluxes from the region with higher entropy toward the lower entropy segments. Figure 7 shows that for all Kn ranges the top left corner of the cavity is where the maximum entropy occurs. Moreover, at Kn=0.05 for the isothermal cavity the entropy reduces from the top left corner toward both the left bottom corner and the right wall, therefore, the heat flux lines originates from the top left corner and are directed toward bottom and right, see figure 6.a.
According to figure 7.c, at Kn =0.5 the only direction for reduction of entropy is from the left wall toward the right wall. As a result, molecules convect the energy from the left cold wall toward the hot right wall. Furthermore, it is seen that as the degrees of rarefaction increases the maximum entropy in domain decreases. Similar distribution of entropy is seen for the adiabatic case. The heat flux lines are originated from the higher entropy regions toward the lower entropy regions in the adiabatic cavity as well. Figure 7.d shows that the heat flux streamlines are denser in the regions where the minimum entropy occurs. Comparison of the isothermal case with the adiabatic cavity shows that the entropy of isothermal cavity is higher than the adiabatic cavity.
In order to study the effects of rarefaction on the molecular velocities, probability distribution functions, PDFs for the isothermal and adiabatic cavity in the top right corner at Kn=0.05 are plotted in figure 8.a. The equilibrium Maxwell-Boltzmann distribution is also shown in this figure. As expected, the predicted flow behaviour by the DSMC deviates from the equilibrium state. Figure 8.a shows that the discrepancies between the velocity distribution functions of the adiabatic cavity and the equilibrium distribution are larger than the isothermal cavity. Figure 8.b shows the comparison of PDF obtained by the DSMC and the equilibrium distribution at the bottom right corner of the cavity. It is seen that as the rarefaction effects decrease at the bottom of the cavity, the PDF approaches to the Maxwell-Boltzmann distribution.

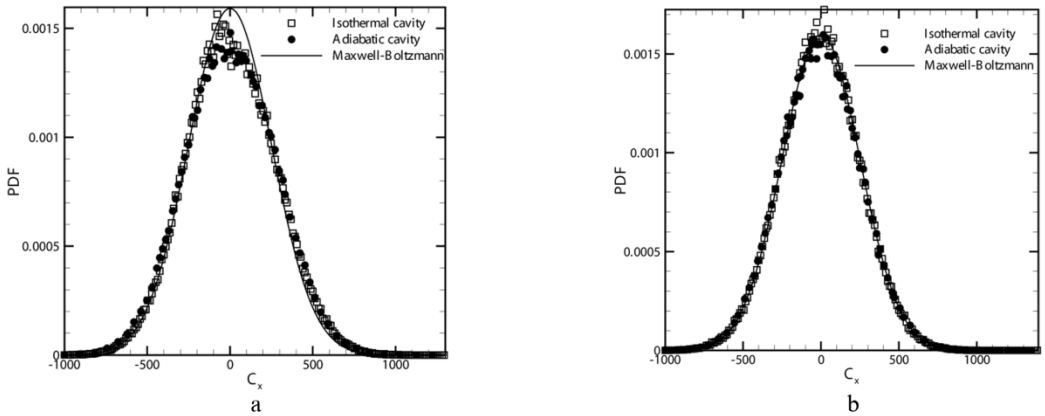

Figure 8: *Comparison of horizontal velocity distribution functions at Kn=0.05, a) top right corner, b) bottom right corner*

We now consider local gradient based Knudsen number, $Kn_{Gl\text{-}Q}$, which is defined as [12]:

$$Kn_{GL\text{-}Q} = \frac{\lambda}{Q_{Local}}|\nabla Q| \qquad (3)$$

where λ is the mean free path and Q represents the local flow quantities such as temperature T, density ρ and velocity magnitude |V|. According to Schwartzentruber et al. [12], Kn_{max}=Max (Kn_{Gl-T}, $Kn_{Gl-\rho}$, $Kn_{Gl-|V|}$) is the proper tool to specify the deviation of the rarefied flow from equilibrium state.

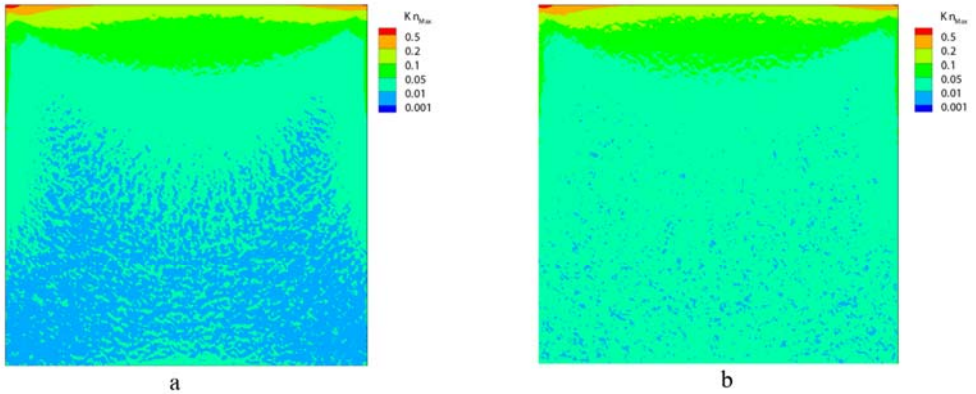

Figure 9: *Distribution of Kn_{max} in the cavity at $Kn_{nominal}$ =0.05, a) isothermal cavity, b) adiabatic cavity*

Figure 9 shows the Kn_{max} distribution in the cavity for the isothermal and adiabatic cavity at Kn=0.05. According to Fig. 9, the non-equilibrium effects are stronger near the top corners. Although in the lower half of the cavity the value of Kn_{max} is below 0.001, the counter gradient heat flux is observed. It leads to this conclusion that the Kn_{Gl} is not a suitable tool for the internal cavity flow. Comparing Figure 9.a with Figure 9.b reveals that the adiabatic cavity strays from the equilibrium state more notably.

Conclusion:

The effect of boundary conditions on the hydrodynamic and thermal characteristic of the micro/nano lid-driven cavity in the slip and transition regime is investigated. It is seen that adiabatic cavity encounters larger temperature rise in comparison with the isothermal cavity. Moreover, compressibility effects are pronounced more significantly for the adiabatic cavity. The directions of heat flux stream lines for both cases are in agreement with reduction of entropy in the flow field. It is also seen that the velocity distribution functions for the adiabatic cavity deviates from the equilibrium Maxwell-Boltzmann distribution more notably in comparison with the isothermal cavity.

References

[1] Bird, G.A., 1994, Molecular gas dynamics and the direct simulation of gas flows, 2nd ed, Oxford university press, Oxford.

[2] Oztop, H.F. and Dagtekin, I., 2004, Mixed convection in two-sided lid-driven differentially heated square cavity, International journal of heat and mass transfer, Vol. 47 (8-9), pp. 1761-1769.

[3] Spasov, Y., Herrero, J., Grau, F.X., and Giralt, F., 2003, Linear stability analysis and numberical calculations of the lid-driven flow in a toroidally shaped cavity, Physics of fluids, Vol. 15 (1), pp. 134-146.

[4] Mizzi, S., Emerson, D.R., and Stefanov, S.K., 2007, Effect of rarefaction on cavity flow in the slip regime, Journal of computational and theoretical nanoscience, Vol. 4 (4), pp. 817-822.

[5] John, B., Gu, X.J., and Emerson, D.R., 2010, Investigation of heat and mass transfer in a lid-driven cavity under non-equilibrium flow conditions, Numerical heat transfer, Vol. 58 (5), pp. 287-303.

[6] Benzi, J., Gu, X.J., and Emerson, D.R., 2011, Effects of incomplete surface accommodation on non-equilibrium heat transfer in cavity flow: A parallel DSMC study, In press, Computers & fluids, Vol.

[7] Roohi, E., Darbandi, M., and Mirjalili, V., 2009, Direct simulation of monte carlo solution of subsonic flow through micro/nanoscale channels, Journal of heat transfer, Vol. 131 (9), pp. 092402.

[8] Darbandi, M. and Roohi, E., 2011, Study of subsonic/supersonic gas flow through micro/nanoscale nozzles using unstructured DSMC solver, Microfluidics and nanofluidics, Vol. 10 (2), pp. 321-335.

[9] Roohi, E. and Darbandi, M., 2009, Extending the Navier–Stokes solutions to transition regime in two-dimensional micro and nanochannel flows using information preservation scheme, Physics of fluids, Vol. 21 (8), pp. 082001.

[10] Mizzi, S., 2008, Extended macroscopic models for rarefied gas dynamics in micro-sized domains, PhD thesis, Department of mechanical engineering, University of strathclyde Glasgow, United Kingdom

[11] Garcia, A.L., 2000, Numerical methods for physics, 2nd ed, Benjamin cummings, Englewood cliffs.

[12] Schwartzentruber, T.E., Scalabrin, L.C., and Boyd, I.D., 2008, Hybrid particle–continuum simulations of nonequilibrium hypersonic blunt-body flowfields, Journal of thermophysics and heat transfer, Vol. 22 (1), pp. 29-37.